AD-A177 090 DEVELOPMENT OF INTEGRAL COATING FOR SOLAR CELL MODULES 1/1
(U) OCLIC/OPTICAL COATING LAB INC SANTA ROSA CA
C D ADAMS DEC 86 AFWAL-TR-86-2095 F33615-82-C-2232
UNCLASSIFIED F/G 11/3 NL

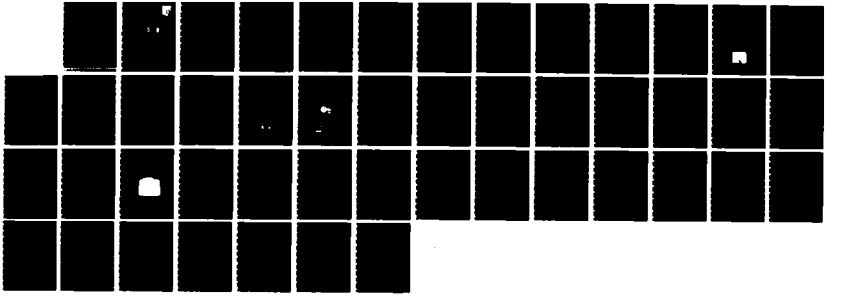

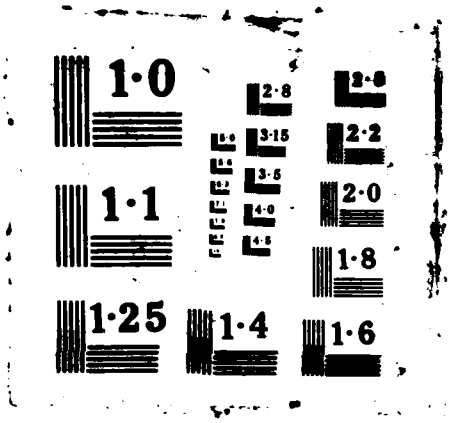
1·0
1·1
1·25
1·4
1·6
1·8
2·0
2·2
2·5
2·8
3·15
3·5
4·0
4·5

AFWAL-TR-86-2095

DEVELOPMENT OF INTEGRAL COATING FOR SOLAR CELL MODULES

Craig D. Adams

Optical Coating Laboratory, Inc.
2789 Northpoint Parkway
Santa Rosa, CA 95407-7397

December 1986

Final Report for Period February 1985 to September 1986

Approved for public release; distribution is unlimited.

AEROPROPULSION LABORATORY
AIR FORCE WRIGHT AERONAUTICAL LABORATORY
AIR FORCE SYSTEMS COMMAND
WRIGHT-PATTERSON AIR FORCE BASE, OHIO 45433-6563

NOTICE

When Government drawings, specifications, or other data are used for any purpose other than in connection with a definitely related Government procurement operation, the United States Government thereby incurs no responsibility nor any obligation whatsoever; and the fact that the government may have formulated, furnished, or in any way supplied the said drawings, specifications, or other data, is not to be regarded by implication or otherwise as in any manner licensing the holder or any other person or corporation, or conveying any rights or permission to manufacture use, or sell any patented invention that may in any way be related thereto.

This report has been reviewed by the Office of Public Affairs (ASD/PA) and is releasable to the National Technical Information Service (NTIS). At NTIS, it will be available to the general public, including foreign nations.

This technical report has been reviewed and is approved for publication.

1Lt ROBERT K. MORRIS
Project Engineer

PAUL R. BERTHEAUD, CHIEF
Power Components Branch

FOR THE COMMANDER

JAMES D. REAMS, CHIEF
Aerospace Power Division
Aero Propulsion Laboratory

"If your address has changed, if you wish to be removed from our mailing list, or if the addressee is no longer employed by your organization please notify AFWAL/POOC-2, W-PAFB, OH 45433-6563 to help us maintain a current mailing list".

Copies of this report should not be returned unless is required by security considerations, contractual obligations, or notice on a specific document.

Unclassified
SECURITY CLASSIFICATION OF THIS PAGE

ADA177090

REPORT DOCUMENTATION PAGE

1a REPORT SECURITY CLASSIFICATION: Unclassified	1b RESTRICTIVE MARKINGS: N/A
2a SECURITY CLASSIFICATION AUTHORITY	3 DISTRIBUTION / AVAILABILITY OF REPORT: Approved for public release; distribution is unlimited.
2b DECLASSIFICATION / DOWNGRADING SCHEDULE	
4 PERFORMING ORGANIZATION REPORT NUMBER(S)	5 MONITORING ORGANIZATION REPORT NUMBER(S): AFWAL-TR-86-2095
6a NAME OF PERFORMING ORGANIZATION: OPTICAL COATING LABORATORY, INC. / 6b OFFICE SYMBOL (If applicable)	7a NAME OF MONITORING ORGANIZATION: AERO PROPULSION LABORATORY, AIR FORCE WRIGHT AERONAUTICAL LABORATORIES
6c ADDRESS (City, State, and ZIP Code): 2789 Northpoint Parkway, Santa Rosa, CA 95407-7397	7b ADDRESS (City, State, and ZIP Code): WRIGHT-PATTERSON AFB OH 45433-6563
8a NAME OF FUNDING / SPONSORING ORGANIZATION: AERO PROPULSION LABORATORY / 8b OFFICE SYMBOL (If applicable): AFWAL/POOC-2	9 PROCUREMENT INSTRUMENT IDENTIFICATION NUMBER: F33615 82 C 2232
8c ADDRESS (City, State, and ZIP Code): WRIGHT-PATTERSON AFB OH 45433-6563	10 SOURCE OF FUNDING NUMBERS: PROGRAM ELEMENT NO 62203F; PROJECT NO 3145; TASK NO 19; WORK UNIT ACCESSION NO 83

11 TITLE (Include Security Classification)
DEVELOPMENT OF INTEGRAL COATING FOR SOLAR CELL MODULES

12 PERSONAL AUTHOR(S)
CRAIG D. ADAMS

13a TYPE OF REPORT	13b TIME COVERED	14 DATE OF REPORT (Year, Month, Day)	15 PAGE COUNT
FINAL	FROM FEB 1985 TO SEP 1986	1986 DECEMBER	44

16 SUPPLEMENTARY NOTATION
N/A

17 COSATI CODES			18 SUBJECT TERMS (Continue on reverse if necessary and identify by block number)
FIELD	GROUP	SUB-GROUP	SOLAR CELLS, SPACE RADIATION EFFECTS, COVER GLASS, SOLAR ARRAY.
22	23	9	
10	01	11	

19 ABSTRACT (Continue on reverse if necessary and identify by block number)

A process has been developed by which integral solar cell covers (ISCC's) can be applied directly to the front surface of solar cell modules. The covers are a codeposited mixture of silica and alumina. The tensile-stressed alumina serves to compensate for the compressive stress of the silica. The process by which these covers are applied is Plasma Activated Chemical Vapor Deposition (PACVD) which is a low-temperature CVD process (145°C). The process utilizes the OCLI-proprietary Plasma Activated Source (PAS) to generate activated oxygen species to simultaneously oxidize silane and trimethylaluminum (TMA) to form silica and alumina on the substrate surface. By adjusting the reactant flow rates, the codeposited cover stress can be adjusted to quite low stress levels, typically zero to three kpsi. Besides serving to protect the pn junction of the solar cells from particle damage, the cover may also serve as an electrical insulator in high-voltage array applications. Tests as to the effectiveness of the integral cover as an insulator will be performed in the
...continued on reverse...

20 DISTRIBUTION / AVAILABILITY OF ABSTRACT	21 ABSTRACT SECURITY CLASSIFICATION	
☒ UNCLASSIFIED/UNLIMITED ☐ SAME AS RPT ☐ DTIC USERS	Unclassified	
22a NAME OF RESPONSIBLE INDIVIDUAL: Lt. Robert K. Morris	22b TELEPHONE (Include Area Code): (513)255-6235	22c OFFICE SYMBOL: AFWAL/POOC-2

DD FORM 1473, 84 MAR — 83 APR edition may be used until exhausted. All other editions are obsolete.

SECURITY CLASSIFICATION OF THIS PAGE

Block 19 Abstract

future by the Air Force. A significant advantage of ISCC's over conventional covers is that the minimum degradation temperature of the assembly is significantly increased by elimination of the adhesive used to bond the conventional covers. In this project, four ISCC modules were delivered: two for the Interaction Measurements Payload for Shuttle (IMPS)/Photovoltaic Array Space Power (PASP) project and two for a Living Plume Shield III (LIPS-III) project.

TABLE OF CONTENTS.

(cont'd)

TABLE OF CONTENTS (cont'd).

LIST OF FIGURES

LIST OF TABLES

1.0 INTRODUCTION

1.1 Objectives

This report documents the development of integral coating for solar cell modules for the Air Force by OCLI. An integral solar cell cover consists of a thick mixed oxide film applied directly to the front surface of a solar cell module. The coating is predominantly silica mixed with a small amount of alumina for stress compensation. The coating is applied using a Plasma Activated Chemical Vapor Deposition (PACVD) process with silane (silicon tetrahydride), trimethylaluminum (TMA) and oxygen as the reactants. The contract is a continuation of previous development work by OCLI for the Air Force which involved deposition of integral covers on silicon and gallium arsenide solar cells.

Integral solar cell covers (ISCC) exhibit significant advantages over conventionally applied solar cell covers including:

- use of ISCC's significantly increases the cells survivability to laser threats by raising the minimum degradation temperature of the assembly by eliminating the adhesive used to bond on conventional covers,
- ISCC's may be much thinner than the minimum thickness for a conventional cover, and thus providing a significant increase in power per unit mass, and
- use of ISCC's eliminates labor intensive cover processing.

The reasons for developing ISCC modules rather than continuing to coat individual solar cells were:

- to reduce the required labor per cell for potential cost savings,
- to allow coating thinner, lighter, more fragile cells which could not be handled individually without substantial breakage, and
- to allow coating of the entire front surface of the assembly (including interconnections between cells, bus bars, etc.) to electrically insulate the solar cell string from the ionized plasma around the satellite in high voltage arrays.

The primary objectives of the current phase of the ISCC module development project were:

- to refine the aluminum-bearing vapor generation, monitoring and metering system,
- to improve the control of the TMA-to-silane ratio to lower coating stress and improve coating reproducibility,
- to develop in situ stress monitoring, if necessary, for low stress reproducibility,
- to increase the coating area diameter to accommodate coating modules rather than individual solar cells, and
- to coat four deliverable modules with acceptable thickness distribution, stress distribution and performance.

All of these objectives were successfully accomplished.

1.2 PACVD coating chamber.

The PACVD process is currently located in Machine 543 at OCLI. This is the same coating chamber that was used during the first phase of this contract. Machine 543 is pumped primarily with a diffusion pump backed by a mechanical pump, but is also equipped with a cold trap to pump water vapor. The reactant flows are controlled with a Unit Instruments mass flow control system. Machine 543 has numerous pressure measuring devices on the chamber including a baratron, a cold cathode gauge, and a convectron gauge. A residual gas analyzer is also installed on the machine. Process temperature is measured by dual thermocouples located on the substrate tooling and is controlled by a quartz heater. Machine 543 is also equipped with an OCLI-proprietary Plasma Activated Source (PAS) for activated oxygen generation.[1,2]

2.0 ISCC MODULE DESIGN.

The ISCC module design, material acquisition, fabrication and characterization were performed for this contract by the Engineering and Test Division, Space and Technology Group of TRW. The modules consisted of a graphite facesheet covered with a Kapton® insulator to which a string of eight solar cells was cemented. The graphite facesheet provided a thermally stable substrate to mount the cells. The Kapton® insulator was required to prevent the solar cell string (which will be biased to ±500VDC) from making electrical contact with the backing plate and spacecraft ground. The eight solar cells were connected in series and cemented to the insulator with DC93-500 adhesive. The solar cell string was terminated on termination strips which were fed through from the front to the backside of the facesheet. A five-wire shielded government furnished cable was connected to the leads for electrical connection with the spacecraft. All the electrical components including the entire front surface of the solar cell string, interconnects, and exposed areas of the termination strips were coated with the integral coating. For the two flight modules, resistance thermal detectors (RTD's) were imbedded into the backside of the graphite facesheet for thermal metrology.

Two deliverable modules were designated for the IMPS project: one diagnostic module (SN304) and one flight module (SN 309). For these modules the graphite facesheet was bonded to an aluminum backing plate which could be mounted directly to the spacecraft. Two deliverable modules were designated for the LIPS III ICA package: one mass module (SN 310) and one flight module (SN 306). The LIPS III modules were bonded to three fiberglass offsets with Heli-Coil® insets instead of the aluminum backing plate. Figure 1 shows a photograph of a coated ISCC module with an aluminum backing plate. Drawings and specifications for the IMPS and LIPS III modules are in Appendix B.

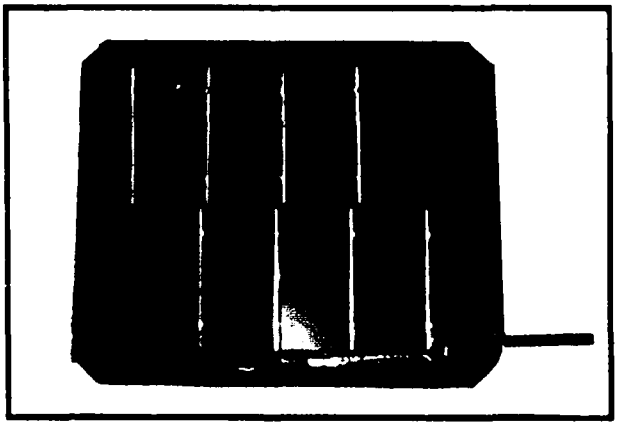

Figure 1: Module (SN 307) after application of integral coating. Five-wire cable has not been attached.

3.0 PLASMA ACTIVATED CHEMICAL VAPOR DEPOSITION (PACVD) PROCESS.

3.1 Characteristics of Integral Solar Cell Covers by the PACVD Process.

Using PACVD for the deposition of integral solar cell covers has a number of significant advantages over other processes:

- stress control may be accomplished by mixing silica and alumina in the proper proportion,
- the process provides for continuous coating with no need to reload sources as is necessary with thermal evaporation,
- deposition rates are currently on the order of 0.1 to 0.3 μm/min with the expectation of significantly higher rates with some equipment modifications,
- the PACVD process produces a low chamber heat load, and
- the PACVD process allows for a relatively low deposition temperature (145°C).

There are some characteristics of the PACVD process that must be considered for safe and proper usage; such as:

- the process is dirty, and considerable measures must be taken to control oxide formation,
- there is a considerable by-product gas load associated with silane cracking that must be pumped away, and
- the reactants are pyrophoric; extreme attention to safe operating procedures and equipment design must be the rule.

3.2 PACVD overview.

An integral solar cell cover is essentially a thick silica coating applied directly to the front surface of a solar cell or solar cell module using PACVD. This is accomplished by causing silane to react to form silica at moderately low temperature (145°C) in the presence of activated oxygen. The source of the oxygen in this process is the OCLI-proprietary Plasma Activated Source (PAS). If pure silica integral covers are deposited, the high stress levels can cause the cells to bend and often break. To compensate for the compressive stress on the solar cell induced by the silica, small amounts of alumina are codeposited with the silica by the oxidation of trimethylaluminum (TMA). Since silica exhibits compressive intrinsic stress and alumina exhibits tensile intrinsic stress, when these two oxides are codeposited in the proper proportion (approximately 12-14 percent alumina), a very low stress film may be deposited.

The PAS source has a cavity in which an RF field is generated. Oxygen is fed through the cavity and a plasma of activated and ionized oxygen species is formed. The activated oxygen is then fed into the chamber through a glass chimney.[3] In the current ISCC process, silane and TMA are introduced into the chamber via a ring-shaped manifold which surrounds the PAS chimney and directs the reactant flow upward toward the substrate (see Fig. 5). The reactants impinge upon the substrate surface where they react to form silica and alumina.

The principal reaction for the oxidation of TMA by the PACVD process is (equation presented unbalanced):

$$Al(CH_3)_3\ (g)\ +\ O_2{}^*\ (g)\ \text{------>}\ Al_2O_3(s)\ +\ C_2H_6\ (g).$$

Methane, ethene and hydrogen may also be produced in this reaction.

The oxidation of silane to form silica on the substrate surface proceeds by the reaction (equation presented unbalanced):

$$SiH_4\ (g)\ +\ O_2{}^*\ (g)\ \text{------>}\ SiO_2\ (s)\ +\ xH_2\ (g)\ +\ yH_2O\ (g)\ .$$

Residual gas analyses were performed which indicate that hydrogen gas, rather than water vapor, appears to be the primary by-product of the silane reaction in the PACVD process. In a series of runs with fixed O_2 flow (20sccm) through the PAS activator at a fixed plasa power, silane flow was varied. It was found that the deposition rate was proportional to the silane flow and that the $H_2{}^{(+)}$ signal on the residual gas analyzer was also proportional to the silane flow. However, it was also found that the $H_2O^{(+)}$ signal was not a function of the silane flow. This strongly suggests that the oxidation of silane in the PACVD process proceeds by the reaction:

$$SiH_4\ (g)\ +\ O_2{}^*\ (g)\ \text{------>}\ SiO_2\ (s)\ +\ 2H_2\ (g)\ ,$$

rather than the reaction:

$$SiH_4\ (g)\ +\ 2O_2{}^*\ (g)\ \text{------>}\ SiO_2\ (s)\ +\ 2H_2O\ (g)\ .$$

In atmospheric-pressure CVD processes (APCVD), it is reported that hydrogen also tends to be the primary by-product of this reaction at low partial pressures of silane and low temperature (< 500°C).[4] However at higher partial pressures of silane and higher temperatures (600°C - 1000°C), it is reported that water becomes the principal by-product.[5] As part of this development contract, a study was done to determine if it was possible and practical to catalytically convert hydrogen to water during the PACVD process. A discussion of this study follows below (see Sect. 4.6).

The desired reaction mechanism for the reactants in the PACVD silane oxidation process is a heterogeneous, surface-catalyzed reaction involving the adsorption on the substrate of the reactants and the subsequent chemical conversion to the desired silica film. It is reported that these reactions generally take place via complex reaction mechanisms involving branching free-radicals.[6] The gaseous by-products then desorb and are pumped away.

Gas phase nucleation of the reactant molecules is also possible via homogeneous gas phase reactions. These reactions result in particles which form a white powder on reactor surfaces. It has not been determined to what extent gas phase reactions occur in the PACVD ISCC process in the substrate zone. It is clear that a substantial amount of silica dust is generated in the chamber particularly in areas away from the substrate zone. For the ISCC process, this dust has not presented a major problem. The substrate faces downward and the surface defects that are observed are not a problem for this product.

Silane is particularly prone to gas phase nucleation.[7] In most higher pressure CVD processes using silane, diluent gases (such as nitrogen) are used to dilute the silane to help suppress gas phase nucleation.[8] This is not practical for the ISCC process , however, because the process is already pumping limited. Alternative silicon-containing compounds are also available including chlorinated silanes up through silicon tetrachloride ($SiCl_4$). The chlorinated silanes are less subject to gas phase nucleation but are also more corrosive and may be more difficult to control.[9]

4.0 PROCESS DEVELOPMENT.

4.1 Aluminum-bearing compound monitoring and metering.

In the first phase of this contract, a number of alternative methods of monitoring and metering the flow of the aluminum-bearing compound were studied. In that phase, triethylaluminum (TEA) was used predominantly as the aluminum-bearing compound. The methods of monitoring TEA were:

- monitor the optical emission lines of a unique TEA by-product with an optical emission spectrometer,
- monitor the mass peak of a unique TEA by-product with a residual gas analyzer (RGA), or
- monitor the total chamber pressure.

The first two methods were problematic due to the degree of noise in the optical emissions and to difficulties with oxide contamination of the RGA detector. Therefore, the second order variable, total chamber pressure, was used to monitor the TEA flow. TEA was metered by either:

- constant aperture, variable temperature, or
- variable aperture, constant temperature.

During the current phase of the contract, the aluminum-bearing compound control system was modified to allow use of a mass flow controller to monitor and meter the flow of the material. TEA's vapor pressure is too low to provide a sufficient pressure differential across a mass flow controller to facilitate the use of a mass flow controller for flow control. Therefore it was required that an acceptable alternative to TEA as the aluminum source material be identified. Trichloroaluminum was considered, but was thought to be potentially too corrosive for the mechanical pump system.

Trimethylaluminum (TMA) was identified as a possible alternative with a sufficiently high vapor pressure for use with mass flow controllers. The vapor pressures of TMA and TEA are presented in Figure 2. A series of alumina films were deposited from TEA and TMA. The alumina films deposited using TMA showed no observable or measurable visible absorption. Estimates of the porosity of the alumina films were also determined spectrally by measurement of the water absorption band in the near infrared. The results of these analyses indicated that less porous films were consistently obtained when using TMA instead of TEA. Based on the results from the single layer tests and subsequent codeposited film testing, it was decided to use TMA for the aluminum-bearing compound in codeposited designs.

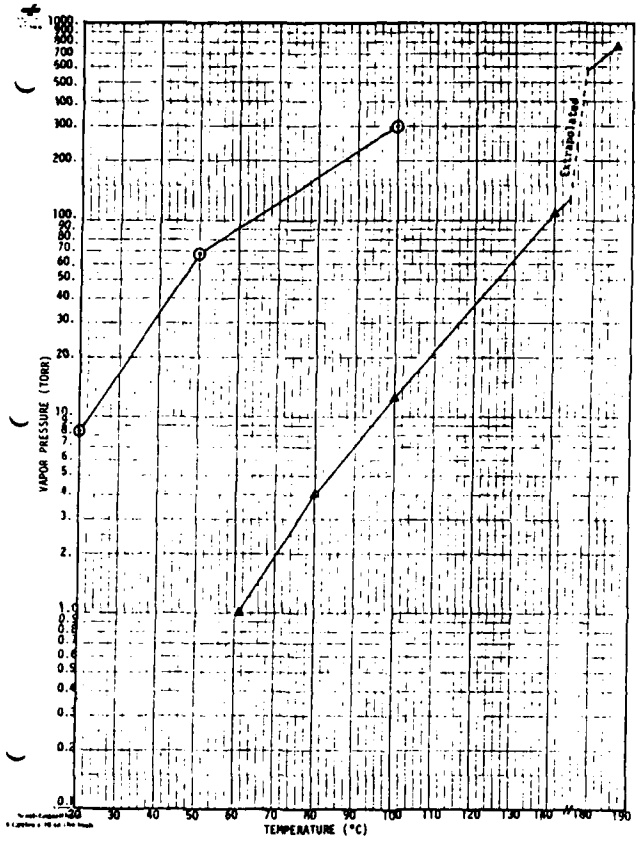

Figure 2: Vapor pressures of trimethylaluminum (TMA) and triethylaluminum (TEA)[10].

The aluminum-bearing compound cannister was placed in a thermostatically controlled oven to raise its vapor pressure. Switching from TEA to TMA as the aluminum-bearing compound allowed the mass flow controller to be placed in the oven used to heat the TMA cannister. This is because the vapor pressure required for stable flow control with a mass flow controller could be maintained at a much lower temperature with TMA than with TEA (36 torr at 41°C for TMA vs. 36 torr at 119°C for TEA). The maximum operating temperature of the mass flow controllers used is 43°C.

Placement of the mass flow controller in the oven also greatly simplified the prevention of reactant vapor condensation in the reactant plumbing. Heating of reactant lines was no longer necessary. This is because the partial pressure of TMA downstream of the mass flow controller, and everywhere outside the oven, is considerably below the vapor pressure of TMA at room temperature. Therefore, no condensation could occur in the reactant lines .

4.2 Elimination of bumping in TMA due to superheating.

A problem was encountered with the superheating of liquid TMA in the cannister and the subsequent bumping or foaming of the liquid TMA into the plumbing. This may have been caused by lack of adequate nucleation when the TMA was heated above its boiling point. Beads were therefore added to the TMA cannisters to provide for adequate nucleation.

Alternatively, superheating may have occurred with sudden decreases in the ambient pressure above the liquid TMA with the flow valve movement. To damp the pressure fluctuations, a surge tank was fabricated and installed above the TMA cannister. The addition of proper nucleation sites and surge suppression apparatus completely solved the superheating problem. The modified TMA vapor generation system is presented in Figure 3.

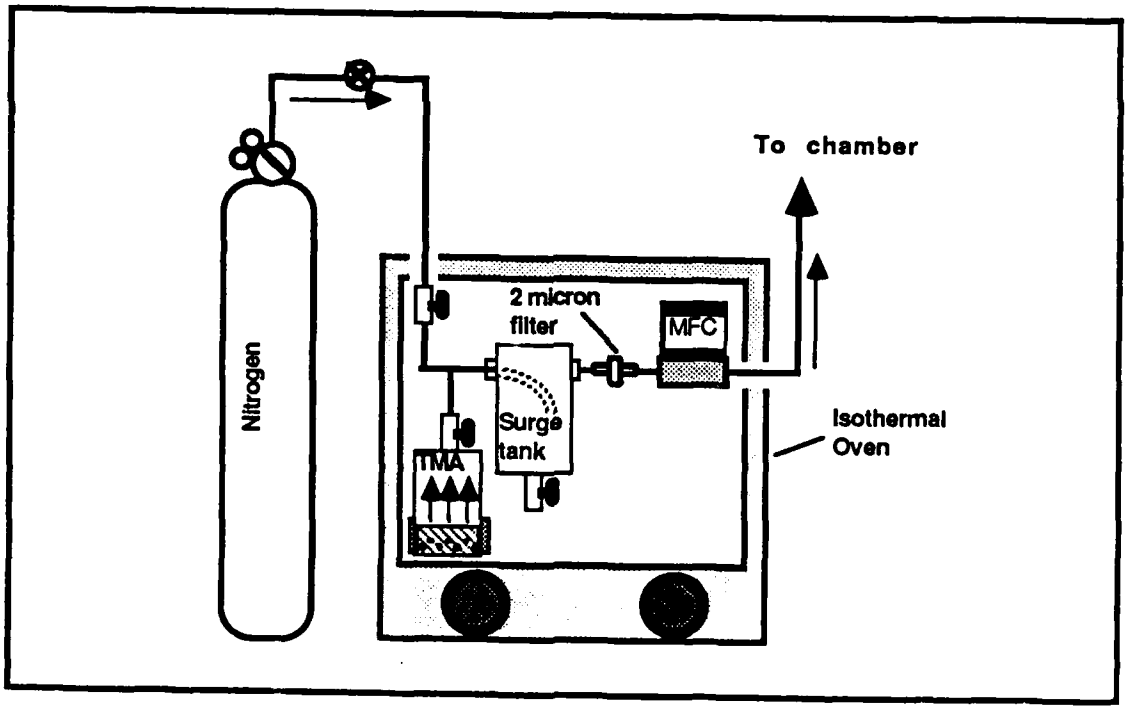

Figure 3: TMA vapor generation system.

4.3 Control of oxide formation in reactant plumbing.

Another aspect of process development addressed was the premature oxidation of silane and TMA in the reactant plumbing. Oxide contamination of sensor and bypass components of the mass flow controllers can cause drifts in the actual reactant flows. Real and virtual leaks in the system were identified. Real leaks were essentially eliminated by switching from Swagelock® fittings to VCR® and welded fittings throughout the system wherever possible. The virtual leak problem was solved by using much more effective purge techniques.

In-line particulate filters in the system also greatly reduced the occurrence of oxide contamination of the mass flow controllers. Reference mass flow controllers were also installed so that drifts in indicated flow rates could be detected, and flow settings adjusted, prior to coating. A schematic of the PACVD is presented in Figure 4.

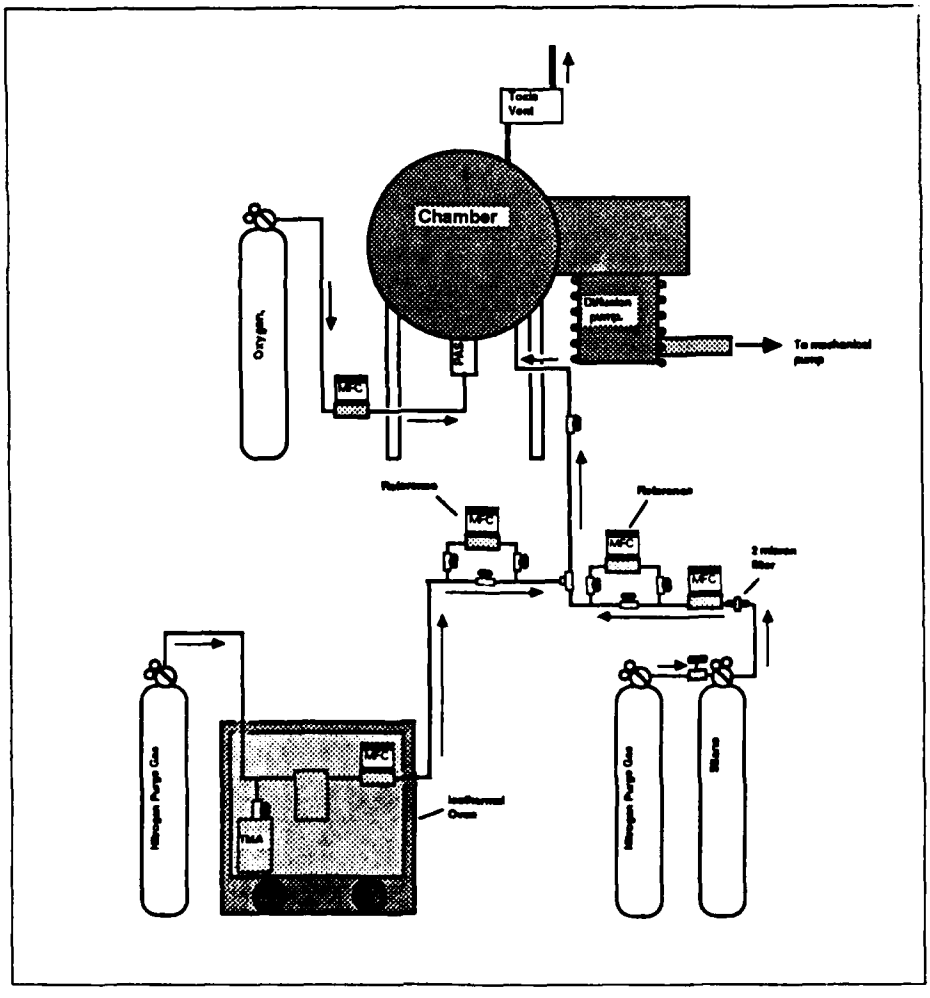

Figure 4: PACVD system configuration for the ISCC process.

4.4 Stress control and in situ stress monitoring.

Due to previous problems related to the monitoring and metering of the aluminum-bearing compound, it had been proposed that in situ stress monitoring would be used to measure the coating stress as it was being deposited. This information would be used in a servo system to control the flow of one or the other reactant gas to maintain the proper stress level. Either a cat's-eye interferometer or a laser distance measuring device was available for this purpose.

Development of stable, reproducible reactant flow controls, however, resulted in the ability to coat very low stress mixed oxide films repeatably without the need for in situ stress monitoring. Therefore in situ stress monitoring was not necessary.

4.5 Expansion of coating area diameter.

During the coating process, the modules were mounted horizontally directly above the PAS chimney in the coating area or zone. A process development required for this phase of the ISCC project was to expand this coating area from about a three or four inch to a six inch diameter to accommodate the larger ISCC modules. Outside of the coating area the film tends to be less dense than the films deposited inside the coating area. A result of the lower density is increased water absorption and swelling of the film causing a compressive shift in film stress once the substrate has been removed from the coating chamber.

To make the stress distribution more uniform, the PAS chimney was modified to expand the activated oxygen distribution and to allow a more uniform radiative heating of the substrate by the plasma. A typical PAS configuration is shown in Figure 5. Mixed oxide films produced using the modified PAS configuration resulted in a significant increase in the coating density at the outside position.

Run	Minumum peak transmission at 2.8μm		PAS chimney type.
	Center location	Outside Position	
543-156	32%	3%	Non-modified
543-157	36%	6%	Non-modified
543-203	36%	36.% (Pos. A) 32% (Pos. B)	Modified

Table 1: Minimum peak transmission at 2.8μm of mixed oxide films coated at the center and outside positions.

Relative porosity of the coatings at the center of the coating area and a position just outside the coating area (3 in. off-center) were deduced by the relative peak heights of the water absorption band at 2.8μm. This data is presented in Table 1 above for the modified and non-modified PAS chimneys.

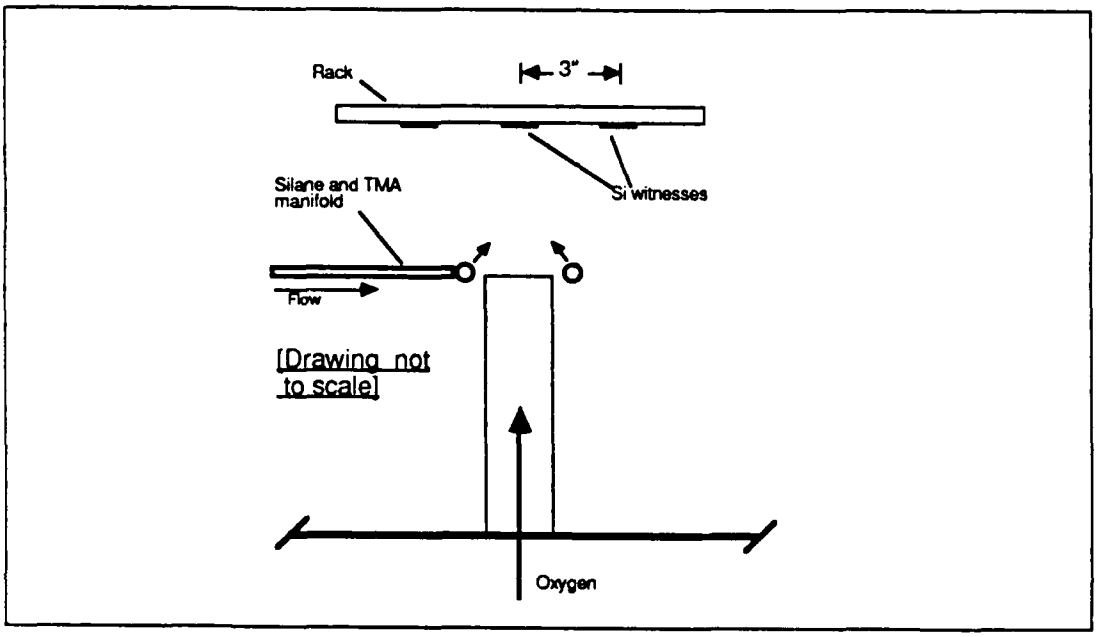

Figure 5: Cross-sectional view of geometry of PAS chimney and substrate rack.

4.6 Catalysis of hydrogen oxidation reaction.

Hydrogen gas rather than water vapor appears to be the primary by-product of the silane oxidation reaction:

$$SiH_4(g) + O_2(g) \text{ ----> } SiO_2(s) + H_2(g) \; [+ H_2O(g)].$$

The diffusion pump on the coating chamber can pump water or hydrogen. The refrigeration trap can also pump water however it cannot pump hydrogen. Since the ISCC machine has both a diffusion pump and a refrigeration trap and since pumping is currently the deposition rate limiting factor, higher deposition rates may be obtained by utilizing a conversion of hydrogen to water. A study was therefore proposed to determine the possible and practical means of oxidizing hydrogen catalytically in the coating chamber during the ISCC PACVD process.

The overall reaction:

$$2H_2(g) + O_2(g) \text{ ----> } 2H_2O(g)$$

can proceed by a number of different mechanisms and it has been shown that either oxygen atoms or protons may initiate the reaction.[11] Although the reaction is generally quite slow at low temperature due to quite high activation energies[12], the rate can be improved by a number of means. If the reactants are at sufficient concentrations, the mixture can explode if ignited. The reaction is quite exothermic so the energy necessary to promote the reaction would come from the reaction itself. In fuel cells the half reactions are catalyzed on metal coatings in the presence of an electrolytic solution such as potassium hydroxide.[13] Fuel cells usually operate in the range from one to ten atmospheres pressure and twenty to one hundred degrees centigrade temperature although some fuel cells operate at much higher temperatures.[14] Additionally, the reaction may be catalyzed by a number of different means, discussed below.

In the case of a bimolecular reaction, the rate of reaction may be increased merely by the presence of solid surfaces (such as the walls of the chamber) due to a concentration factor.[15] This is because the concentration of the reactants may be higher in the surface film than in the gas phase. Secondary surface structure, such as edges, corners, grooves, etc., located on fixtures and walls in the chamber also can be an important factor.[16]

Some work with photosensitization of the oxidation of hydrogen reaction using metal vapor such as mercury has been done.[17] Rate increases were observed and were probably due to initiation of the reaction by initial reactions between the mercury atoms and hydrogen.[18] A process of this type would, however, likely cause contamination of the growing silica film.

Heterogeneous catalysis using a solid catalyst was another consideration. It has been shown that the reaction may be catalyzed on platinum, nickel and palladium, as well as some other materials, by lowering the activation energy required.[19,20,21] The mechanism for the catalysis can be dissociative adsorption, or possibly chemisorption, of one or both reactants on the surface of the catalyst. Nickel and palladium, however, can eventually become poisoned by exposure to oxygen by oxide formation on the surface.[22] Thus, platinum or a platinum complex would probably be the metal of choice for catalyzing the reaction. One problem with the use of a platinum catalyst in the ISCC process is that the reaction rate at 145°C is quite slow.

A number of means of introducing fresh platinum or nickel surfaces to the machine were considered. The most efficient means of supplying the initial catalytic surfaces and of regenerating fresh catalytic surfaces during the run was thermal evaporation of platinum or nickel from an electron beam source. Operation of this source would require lower chamber pressures than those used during ISCC deposition. Thus, deposition of coating on the substrate would have to be suspended each time a new catalytic surface was to be generated. Additionally, ISCC film contamination might be a problem as might oxidation of the catalyst before deposition on the chamber walls.

Since the process operates in a relatively low vacuum and has a high deposition rate, essentially every surface in the chamber rapidly becomes coated due to scattering of the silica and alumina flux. If one assumes that one hundred angstroms of coating is sufficient to substantially inhibit all catalytic activity, then within seconds, or at least a few minutes, any catalytic rate enhancement would cease. Unfortunately, regeneration of the catalyst every few minutes would severely impact the coating time and process.

If one were to assume that fresh platinum or nickel surfaces could be maintained, then to predict the rate enhancement that would be achieved would require knowledge of the exact mechanism(s) by which the reaction would proceed. One possible mechanism on a nickel or palladium catalyst might be:

(1) $O_2(g)$ ----> $O(ads) + O(ads)$

(2) $O(ads) + H_2(g)$ ----> $H_2O(ads)$

(3) $H_2O(ads)$ ----> $H_2O(g)$

Other more complex mechanisms involving cleavage of the molecular hydrogen-hydrogen bond and with hydroxyl ($(OH)^-$) and peroxyl ($(HO_2)^-$) group intermediates are also possible but will not be detailed here.[23] It appears evident, however, that the conversion of hydrogen to water on a solid catalyst would involve a number of different mechanisms proceeding simultaneously. From the reaction mechanisms and assumptions regarding the rate limiting steps, the kinetic rate equations for the reactions may be derived using the Langmuir-Hinshelwood method for heterogeneous reactions. This method takes into account adsorption and surface reactions in a consistent manner. Rate constants, however, must be determined experimentally.

In conclusion, it was determined that there are a number of means with which the reaction:

$$2H_2(g) + O_2(g) \text{ ----> } H_2O(g)$$

may be catalyzed. Unfortunately, none of these means are compatible with the PACVD process for deposition of integral solar cell covers.

4.7 Process parameters.

Typical values for temperature, pressure, rate and reactant flow rates are listed in Table 2. A range of values for the same parameters for depositing mixed oxide coatings generally with the PACVD process are also listed in Table 2 for comparison. Some parameters such as temperature were limited by substrate material. Mass flow rates were limited by available pumping and affected the process pressure. The deposition rate was a function of the system geometry and mass flow rates.

It may be seen that to coat a 0.003 in. cover the actual coating time was in excess of six hours. Additionally, there was about a two hour heat soak at the beginning of each run and a two hour minumum purge time at the end of each run. Automation of certain aspects of this process would therefore be desirable particularly in a production mode. An alarm system could alert a technician to significant changes in process parameters, such as:

- reactant flow rate (due possibly to a reactant bottle emptying),
- process temperature,
- process pressure, or
- instabilities or extinguishment of the PAS plasma.

Data-logging could also be periodically performed to log all significant process parameters. Currently a technician monitors and logs process parameters but rarely needs to take any action.

The process parameters for the ISCC process have not been fully optimized. For example, it is expected that substantially higher deposition rates may be obtained with higher mass flow rates.

Parameter	Typical	Range
Temperature	145°C	25°C - 500°C
Pressure	1.5 mtorr	0.5 mtorr - 10.mtorr
Rate	0.2 µm/min	0.1 µm/min - 1.0 µm/min
Reactant mass flows:		
Oxygen	37. sccm	Varied.
Silane	100. sccm	Varied.
TMA	13. sccm	Varied.

Table 2: Range of values for deposition of mixed oxide films and typical values for deposition of integral solar cell covers by PACVD.

5.0 INTEGRAL SOLAR CELL COVER COATING RESULTS.

5.1 Thickness distribution.

The required coating area for the integral solar cell cover module extends to a 2.5 in. radius around the center of the PAS. While the specifications call for a film thickness of from 0.002 in. to 0.006 in., it was desired to limit the coating run-off to about thirty percent or less . To achieve this, the rack height above the PAS chimney and gas manifold was set at from 6 in. to 8 in. with the initial PAS configuration. Once the modified PAS configuration was developed, the rack height remained at 6 in.

With the initial PAS configuration and gas manifold, the mixed oxide film thickness runoff to 3.0 in. off-center averaged twenty to thirty percent at 6.0 in. and 8.0 in. rack heights, respectively. Use of the modified PAS configuration and gas manifold reduced the ISCC average thickness runoff to typically less than 10-15 percent (Fig. 6). The system geometry of the PAS chimney and gas manifold was presented in Figure 5. Thickness measurements were generally made using a Tencor Alpha Step profilometer.

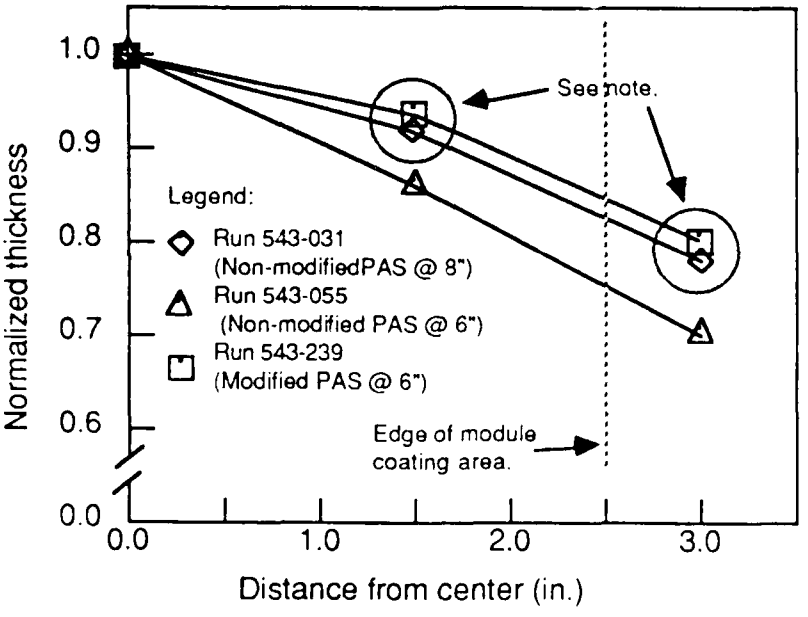

Figure 6: Thickness profile for coatings deposited by PACVD with non-modified and modified PAS configurations. Porosity of coating at outside position was significantly less with modified PAS than with non-modified PAS.

5.2 Stress distribution.

By adjusting the TMA-to-silane flow ratio, the stress level of the resulting mixed oxide covers could be set to the desired stress level. Coatings that were too tensile were occasionally observed to pull apart and craze. For this reason the coating was typically applied with a slight compressive stress, generally 1 - 3 kpsi at the center location and slightly higher at the outside location. The intrinsic stress distribution of coatings from three runs with different TMA-to-silane ratios is presented in Figure 7.

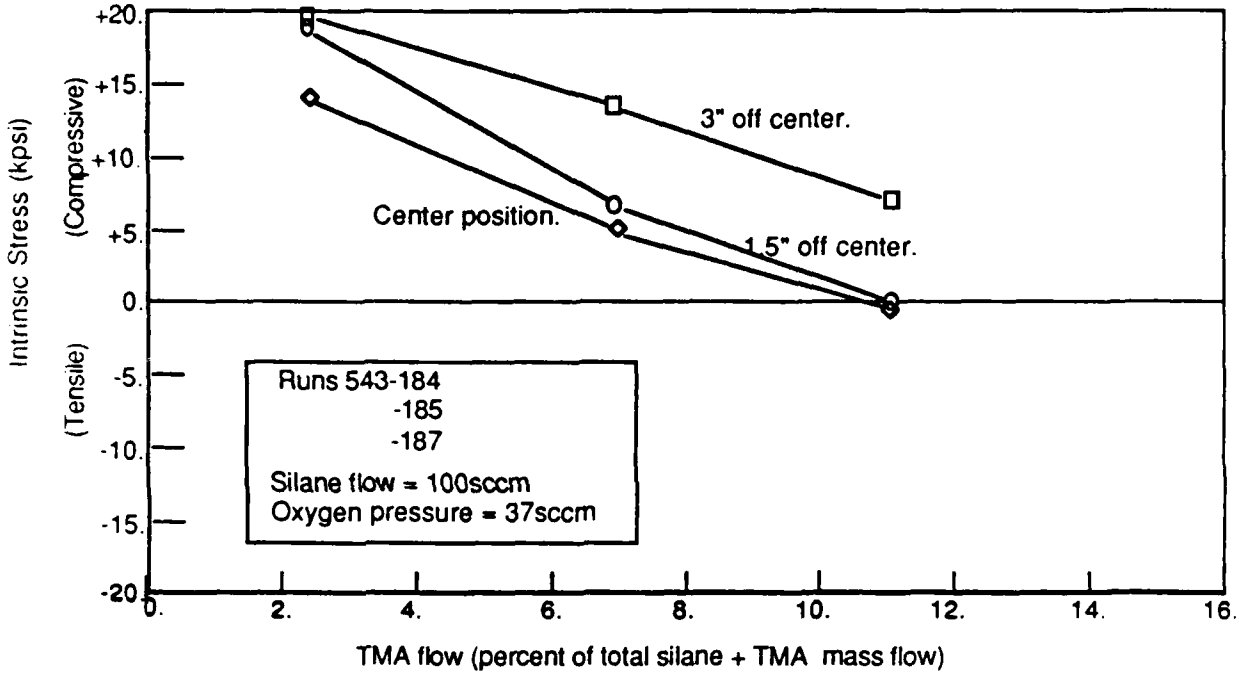

Figure 7: Intrinsic stress distribution of codeposited silica/alumina films with increasing TMA-to-silane ratio.

Stress measurements were made on 0.040 in. silicon stress witnesses using an OCLI-designed stress interferometer. The stress in a coating was determined by measuring the curvature of the coated part in the stress interferometer.

The OCLI stress interferometer consists of an optical system which measures the curvature of a witness due to coating stress. A laser beam illuminates the sample as it sits above a reference flat. The light is reflected and forms interference patterns which may be viewed on a screen or photographed. The primary fringes are those due to interference between the bottom (coated side) of the witness and the top of the reference flat. These fringes indicate the curvature of the part.

The magnitude of the film stress may be calculated using the formula:

$$\sigma = [K \cdot t_s^2 \cdot n] \ / \ [t_f \cdot \rho^2]$$

where:

t_s = substrate thickness,

t_f = coating thickness,

n = number of fringes,

ρ = radius of coated area on substrate, and

K = *f* (Poisson's distribution of the substrate, Young's modulus of the substrate).

The sign (tensile or compressive) of the film stress could be determined by observing the direction that the fringes appear to move on the interferometer's viewing screen as the substrate is tilted.

5.3 Coating porosity.

The mixed oxide films all had some porosity associated with them as evidenced by water absorption lines at 2.8μm in the infrared. The magnitude of the 2.8μm peak was indicative of the relative amount of water that was in a film. When corrected for film thickness, the 2.8μm peak was also a good measure of the relative porosity of a film and served as a useful tool in process development. The minimum peak transmission at 2.8μm for a typical film was presented in Table1.

5.4 Coating composition analysis.

The silicon-to-aluminum ratio of witnesses coated at the center and outside position in run 543-187 was determined at OCLI using Energy Dispersive X ray technique on a Scanning Electron Microscope. The composition of the film was determined to be 22.% aluminum and 78.% silicon at both the center and outside positions. This corresponds to a film composed of 12.4% alumina and 87.6% silica. The stress levels for these films are presented in Figure 7.

5.5 Electro-optical testing results.

The deliverable modules were electro-optically tested at TRW before and after application of the integral cover at OCLI. The current vs. voltage (I-V) curve results of these tests are presented in Appendix A. The short circuit current (I_{SC}), open circuit voltage (V_{OC}), and fill factor (FF) measured before and after application of the ISCC on each deliverable module is presented in Table3. Some apparent degradation in short circuit current (I_{SC}) was measured in each of the deliverable modules. There was no degradation in open circuit voltage (V_{OC}) however, and an actual increase in fill factor (FF) in each module. Fill factor is defined as the maximum power of the cell divided by the product of the short circuit current and the open circuit voltage. The fill factor for module SN 304 before coating is presented in Figure 8.

A degradation in short curcuit current combined with no change in open circuit voltage is almost always indicative of optical losses outside the cell itself according to project engineers at TRW, Engineering and Test Division, Space and Technology Group, who performed the electro-optical testing. There are two optical losses that may be accounted for in this system:

- lack of antireflection coating on integral cover, and
- edge delamination of integral cover.

The initial measurements were performed on cells with an anti-reflection (AR) coating matched to the index of the cover. When the modules were remeasured however, the air interface had no AR coating because the integral cover had been applied over it. The reflection off the solar cell surface was therefore about two percent higher in the after-coating electro-optical tests. The edge delamination of the coating from the cells is discussed in Section 5.7. In areas where the coating has delaminated at the edge of the cell, the reflection off the top surface is higher than in other areas, thus causing an optical loss to occur.

Module SN	V_{oc} (VDC)			I_{sc} (ma)			FF (%)		
	Before	After	% Change	Before	After	% Change	Before	After	% Change
SN 304	4.33.	4.34.	0.0	289.	274.	-5.2	75.7	77.8	+2.8
SN 306	4.35	4.36	0.0	288.	258.	-10.4	78.6	79.7	+1.4
SN 309	4.35	4.35	0.0	291.	254.	-12.7	77.1	81.5	+5.7

Table 3: Electro-optical test results for deliverable ISCC modules (see also Appendix A).

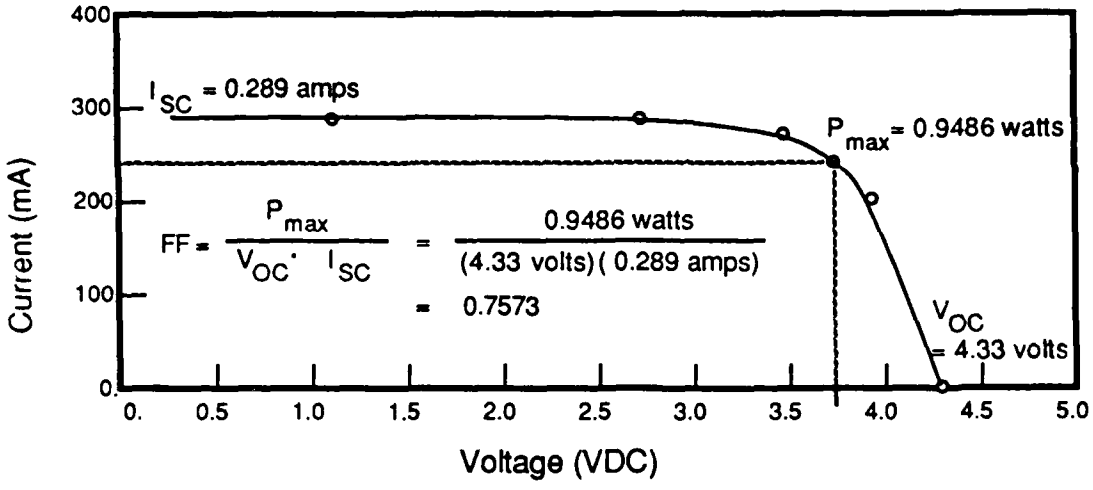

Figure 8: I-V curve of module SN 304 before application of ISCC. Schematic representation of fill factor (FF) is shown.

5.6 Standard environmental test results.

Some environmental testing was performed on the integral solar cell cover coating outside the statement of work. ISCC coatings were applied to samples of all the materials to be coated on the actual module. The results of these tests are presented in Table 4.

Test \ Material	Silicon	AR'd solar cell	Silver-coated Invar	SN62-coated Invar	Press'd SN62 on SC	DC93-500 Adh.	Kapton
1) Snap tape test.	Pass	Pass	Pass	Pass	Pass	Pass	Pass
2) Temperature cycle (-50°C to +100°C, 2 cycles)	Pass	Pass	Pass	Pass	Pass	Pass	Pass
3) 100 eraser rub.	Pass	Pass	Pass	Pass	Pass	Pass	Pass

Table 4: Environmental test results for mixed oxide films on module materials.

Some films were additionally subjected to humidity and post-humidity tape tests. All silicon witnesses and silicon solar cells with antireflection coatings which were submitted passed humidity testing. Some humidity test failures were observed on module materials other than silicon and silicon solar cells with antireflection coatings. For this reason, it is recommended that the modules be stored in a dry nitrogen environment for long term storage.

5.7 Surface contamination of module solar cells.

A problem of edge delamination of the mixed oxide cover was encountered on some solar cells on module assemblies. This problem was unexpected because:

- no such delamination occurred on the numerous individual solar cells that were coated with integral covers, and
- delamination of the integral coating did not occur on the individual module materials as discussed in Section 5.6.

The edge delamination did not occur until the chamber was opened. The coating was then observed to separate at the edges only on some of the module's cells. Every module had some cells exhibiting this effect. The separation was not exhibited on interconnects, Kapton®, or the adhesive. Usually the affected area was at the cell edge away from the bus-bar. A module exhibiting this effect is shown in the photo in Figure 9. The coating in the laminated area could not be removed by a tape test.

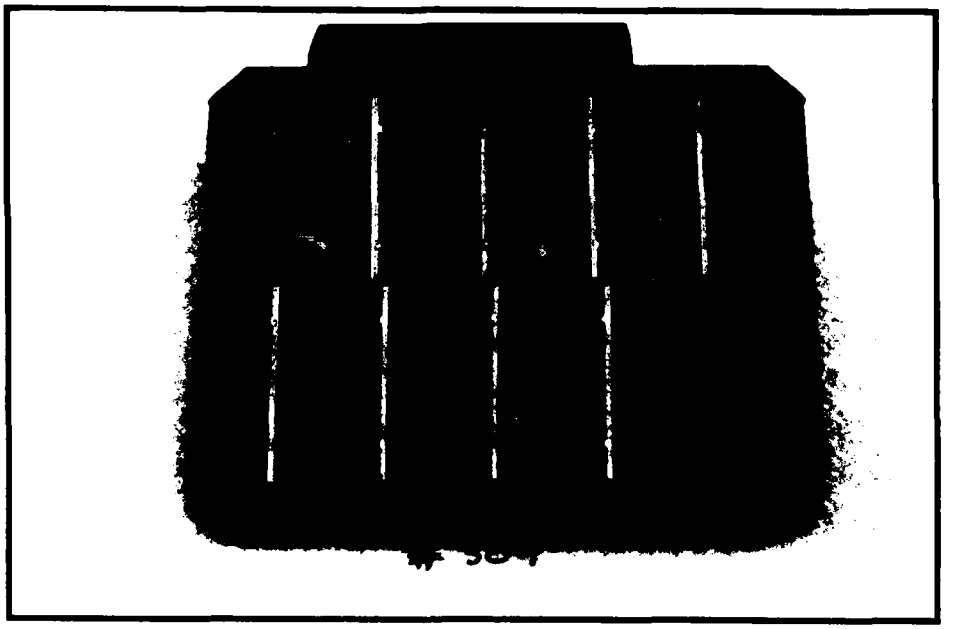

Figure 9: Photograph of solar cell module (SN 304) exhibiting delamination of integral cover along edge of some solar cells.

It was thought that the cause of the edge delamination is due to surface contamination from one of the following sources:

- the DC 93-500 adhesive used to bond the cells to the Kapton® insulator,
- the silicone adhesive on the Kapton® insulator, or
- residual solder flux that may have remained in the solder after the solar cell string was assembled and cleaned.

There were a number of possible mechanisms by which the solar cells may have become contaminated. These mechanisms include:

- the contaminant may have intruded onto the solar cell surface during fabrication of the modules and the cleaning method used did not effectively remove it,
- the contaminant may have intruded onto the solar cell surface during cleaning by the transfer of the DC93-500 adhesive that the cell is imbedded in,
- the contaminant may have outgassed and redeposited onto the solar cell surface while the modules were being brought up to coating temperature and outgassed, or
- the contaminant may have creeped onto the solar cell surface while the modules were being brought up to coating temperature and outgassed.

The cleaning sequence used to clean the modules was to wipe the modules with:

- acetone or methyl ethyl ketone (MEK),
- then trichloroethane, and
- then high purity ethanol.

There were stains on the solar cells that could not be removed. Some stains were only apparent at high angles of incidence, while others reflected violet colors by interference effects.

In an attempt to determine the source of the problem and possible solutions, some additional testing and analysis was performed independent of the project itself. It was thought that this information should be pursued for future planning purposes. Three tests were performed:

- Auger analysis of experimentally contaminated samples,
- lower temperature coating, and
- argon scrub of solar cells.

The Auger analysis experiment consisted of cementing 1 in. diameter germanium witnesses to glass plates using either DC93-500 adhesive or Kapton® tape with a silicone adhesive as was used on the modules. Two of each type were made up (four samples total). Then one of each type was cleaned by the aforementioned procedure and submitted for Auger analysis. The remaining two samples were also cleaned by the same method and then baked in the coating chamber at the process temperature (145°C) for two hours. The samples were then removed and submitted for analysis. Additionally, a reference germanium witness was similarly cleaned and submitted.

The results of the Auger analysis are presented in Table 5. These results seem to indicate that any silicones on the substrate are being substantially removed prior to coating, but then are being redeposited on the surface by either a creep or an outgassing mechanism, particularly at the edges. It may also be possible that solder flux contamination was contributing to the problem but this was not studied due to time constraints.

Sample	Cleaned only		Cleaned and baked.	
	Edge	Center	Edge	Center
Germanium on DC93-500	3.0	3.5	10.0	SD
Germanium on Kapton.	2.5	2.0	11.0	4.0
Germanium reference.	ND	ND	NA	NA

ND = Not Detected NA = Not Analyzed SD = Sample Damaged

Table 5: Relative Auger peak heights from Auger analysis of germanium test samples.

Two other tests were performed to see if the contamination effect could be reduced. Sample coatings were made at a process temperature of 100°C instead of 145°C to reduce potential creep and outgassing. The results were very poor adhesion generally of the coating to test solar cells. Another test was performed to see if solar cells could be glowed in an argon plasma prior to coating to activate the surface and enhance adhesion. Oxygen was not used because that would have caused oxidation of the silver interconnects. Two solar cells were electro-optically characterized and then glowed in argon for two and ten minutes, respectively. The cells were then recharacterized. The tests showed that the cells did indeed degrade (see Table 6). Therefore, neither of these procedures was included in the coating procedure.

It is strongly recommended that the source of the delamination be identified and eliminated in future module designs. It is also suggested that in future module designs solar cells be spot welded rather than soldered and cemented to a Kapton® insulator. This would eliminate the solder , solder flux and the adhesives from the module assembly.

Cell #	V_{oc} (mv)			I_{sc} (ma)			FF		
	Before	After	% Change	Before	After	% Change	Before	After	% Change
#1 (glow)	605.	597.	-1.3	101.5	100.3	-1.2	78.6	77.9	-0.9
#2 (glow)	604.	595.	-1.5	101.1	100.2	-0.9	78.6	77.6	-1.3
#3 (ref)	601.	595.	-1.0	100.2	99.2	-1.0	79.5	79.7	+0.3
#4 (ref)	602.	597.	-0.8	100.2	99.6	-0.6	79.5	79.9	+0.5

Table 6: Electro-optical results of argon glow tests of silicon solar cells.

5.8 Results of qualification testing per statement-of-work.

The statement-of-work requires the following qualification tests:

a) 25 excursions of temperature in dry air from -50°C to 100°C, with a minimum temperature increase rate of 30°C per minute.

b) Vibration test according to IMPS flight acceptance requirements (two tests: random vibration testing and sinusoidal vibration testing).

c) Electo-optical testing for degradation.

The environmental module passed all qualification tests. The results of these tests are listed in Table 7. All tests were performed and certified by TRW, Engineering and Test Division, Space Technology Group. The temperature cycle and vibration test specifications are listed in Appendix C. The electro-optical results are listed in Section 5.5 and in Appendix A.

Test	Result
1) Temperature cycle. (46 cycles (25 required), -50°C to +100°C))	Pass
2a) Random vibration test.	Pass
2b) Sinusoidal vibration test.	Pass

Table 7: Results of qualification testing of environmental test module (SN 303).

6.0 SUMMARY.

In summary, the primary objectives of this phase of the development of integral coating for solar cell modules have been achieved. These achievements include:

- development of the TMA system so that a stable, reproducible TMA flow is maintainable,
- low stress (typically, 0 - 3 kpsi) mixed oxide coatings can be reproducibly applied by proper monitoring and control of the TMA-to-silane ratio,
- in situ stress monitoring is no longer necessary because of the reproducibility of the process and the coatings,
- the coating area was enlarged sufficiently to coat the ISCC modules, and
- the four deliverable modules were coated with integral solar cell covers with acceptable thickness and stress distributions.

The determination of the effectiveness of the covers in insulating the high voltage solar cell array from the space plasma must await the diagnostic module tests, and the actual flight test.

Some problems with edge delamination on some module solar cells were encountered. The problem was not apparent when individual cells were coated. Tests were performed and documented which indicate the source of the problem may be surface contamination by silicones from the DC93-500 adhesive and the Kapton® adhesive. These problems may be engineered out of follow-up module designs as was discussed previously.

7.0 RECOMMENDATIONS.

The current development phase of the PACVD process for the application of solar cells has been successfully completed. This section addresses recommendations for future directions for the ISCC technology. The recommendations may be divided into three areas:

- upgraded solar cells,
- alternative materials, and
- scale-up of the ISCC PACVD process.

7.1 Upgraded solar cells.

It appears that the trend in solar cells is toward more efficient and thinner cells. Gallium arsenide (GaAs) solar cells have potential advantages over silicon solar cells in that:

- GaAs solar cells typically are more radiation resistant than silicon cells and therefore may have a longer life in the space environment,
- GaAs solar cells typically have higher efficencies than silicon cells, and
- GaAs solar cells may have significant weight per power advantages over silicon cells because they may be made thinner with equal power output when applied to a foreign substrate such as germanium.

It is therefore recommended that the application of integral solar cell covers to gallium arsenide (GaAs) solar cells specifically and to thinner cells generally be pursued. Since GaAs solar cells are more brittle than similar silicon solar cells and therefore more subject to breakage, it may be necessary to further reduce the reproducible cover stress "window" from about 0 - 3 kpsi to some smaller value. This may require modifications to the current PACVD process, such as:

- increased use of computers in process monitoring and control, and
- improvements to the gas flow system and equipment.

Further significant improvements in coating reproducibility and lower cover stress may be attainable by periodic, automatic reference reactant flow checks and corrections to reactant flow rates. This procedure might only take a few minutes and could be performed every hour or so with insignificant impact to the coating time. Another recommendation regarding process automation is to develop alarm and data-logging capabilities. Currently a technician monitors and logs process parameters but rarely needs to take any action over the six to eight hour coating run. The alarm system could alert a technician to significant changes in process parameters, such as:

- reactant flow rates,
- process temperature,
- process pressure, or
- instabilities or extinguishment of the PAS plasma.

By automating the monitoring and data-logging aspects of the PACVD process, significant cost

reductions may be realizable even in development phase activities.

A number of means of significantly improving the reactant plumbing system have been identified and it is recommended they be included in future system specifications and upgrades. These modifications include:

- identification and acquisition of mass flow controllers with better field maintainability than those currently being used,
- specific improvements to the purge systems and procedure, and
- specific modifications to reactant plumbing to reduce virtual leaks.

These measures are directed at improving and lowering the reproducible stress profile by reducing the oxide formation in the reactant plumbing and mass flow controllers. This would reduce drifts in reactant flow rates so that the ratio of the reactant gases may be held to a tighter tolerance.

7.2 Alternative materials.

It is recommended that the use of alternative materials in the ISCC PACVD process be pursued. The use of alternative materials for this application may result in a less complex process and films with:

- improved film quality (less scatter, less surface defects, etc.)
- increased film density, and
- decreased oxygen permeability.

For example, a potential alternative low stress integral cover mixture is silica doped with silicon nitride for stress compensation. During this development effort deposition of silicon nitride was accomplished using silane and molecular nitrogen as the reactants. However, the rates that were achieved were too low to allow reasonable cover deposition rates. Since ammonia is significantly more reactive than molecular nitrogen, ammonia is a potentially better alternative source of atomic nitrogen if activated along with oxygen in the PAS unit. If the silica/silicon nitride combination could be successfully coated at adequate rates and film characteristics, the system could be significantly simplified by elimination of the TMA gas handling system. It is recommended that this mixture be investigated for use as the integral cover mixture.

Other alternative materials for the ISCC PACVD process include the chlorinated silanes. The chloronated silanes have a reduced tendency toward gas phase nucleation compared with silane which is currently used in this process. If gas phase nucleation were reduced, it is expected that coatings with less optical scatter (due to fewer surface defects), increased film density and decreased porosity may be obtainable.

Due to time and budgetary constraints, few alternative materials were studied in previous development phases. It is therefore strongly recommended that some of these alternatives be studied for their applicability to the ISCC PACVD process.

7.3 Scale-up of the ISCC PACVD process.

Although the current integral solar cell cover product is probably not ready for scale-up, issues regarding scale-up are still being considered. One issue regarding scale-up of the ISCC process that must be addressed before a production type machine can be designed regards the placement of multiple PAS units in close proximity to each other in the PACVD process. Some work with multiple PAS units in a single coating chamber is currently being performed at OCLI. From this work, important information regarding equipment issues and multiple plasma source interactions (with potential plasma instabilities) is being acquired. Other questions specific to the ISCC process cannot be answered in the current non-CVD muliple PAS machine. Therefore it is recommended that a PACVD machine be equipped with multiple PAS sources to determine:

- effects on coating characteristics such as porosity and scatter,
- required measures to reduce effects of cross-talk between sources on the ISCC coating if necessary.

Unfortunately the current PACVD machine used for the application of ISCC coatings (machine 543) is too small to accommodate multiple PAS units.

Another issue regarding scale-up of the PACVD process is to determine the best methods of increasing the pumping capacity of the system to accommodate increased gas loads that would accompany higher rate coating. This may entail larger or multiple diffusion pumps, increase use of cryogenic pumping or even use of alternative reactants that may produce a smaller volume of by-products.

REFERENCES

1) Gurev, Harold S., "Method and Apparatus for Forming Films from Vapors using a Contained Plasma Source," U.S. Patent # 4,268,711, May 19, 1981.

2) Gurev, Harold S., "Method and Apparatus for Forming Thin Film Oxide Layers using Reactive Evaporation Techniques," U.S. Patent # 4,361,114, May 19, 1981.

3) *Ibid.*

4) Ban, Vladimir S., and Kern, W., Ed., "Chemical Vapor Deposition of Inorganic Thin Films," from Vossen, John L., and Kern, W., Ed., *Thin Film Processes*, Academic Press, Inc., pg.302.

5) *Ibid.*, pg.302.

6) Ban, Vladimir S., and Kern, W., Ed., "Chemical Vapor Deposition of Inorganic Thin Films," from Vossen, John L., and Kern, W., Ed., *Thin Film Processes*, Academic Press, Inc., pg.302.

7) *Ibid.*, pg.302.

8) *Ibid.*, pg.306.

9) Kamins, Ted, "Chemical Vapor Deposition (CVD)," Education Committee American Vacuum Society, pg. 23.

10) Misc. sources.

11) Noyes, W.A. Jr. and Leighton, P.A., The Photochemistry of Gases, Dover Publications, Inc., New York (1966), pgs. 236-237,249-253.

12) *Ibid.*

13) Mantell, C.L., Batteries and Energy Systems, McGraw-Hill Book Company, New York (1970), chapter 7.

14) Alberty, R.A., Physical Chemistry, John Wiley and Sons, New York (1980), pgs. 184-186.

15) Adamson, A.W., Physical Chemistry of Surfaces, John Wiley and Sons, New York (1976), pg. 666.

16) *Ibid.*

17) Noyes, W.A. Jr. and Leighton, P.A., The Photochemistry of Gases, Dover Publications, Inc., New York (1966), pgs. 236-237,249-253.

18) *Ibid.*

19) Latimer, W.M., The Oxidation States of the Elements and their Potentials in Aqueous Solutions, Prentice-Hall, Inc., Englewood Cliffs, N.J. (1952), pg. 34.

20) Boreskov, G.K., Interaction of Gases with Surfaces of Solid Catalysts (from Fundamentals of Gas-Surface Interactions) (1967)

21) Smith, J.M., Chemical Engineering Kinetics, McGraw-Hill Book Company, New York (1981), pgs. 350-356.

22) Boreskov, G.K., Interaction of Gases with Surfaces of Solid Catalysts (from Fundamentals of Gas-Surface Interactions) (1967)

23) Noyes, W.A. Jr. and Leighton, P.A., The Photochemistry of Gases, Dover Publications, Inc., New York (1966), pgs. 236-237,249-253.

APPENDIX A

Current-voltage results of electro-optical testing by TRW, Engineering and Test Division, Space Technology Group, on deliverable modules.

Module: SN 306

Before coating.		After coating.	
Voltage (Vdc)	Current (mA)	Voltage (Vdc)	Current (mA)
4.35 V	---	4.36 V	---
3.92	229. mA	3.92	209. mA
3.83	247.	3.83	225.
3.74	260.	3.74	238.
3.60	273.	3.60	249.
3.47	281.	3.47	254.
3.16	287.	3.16	256.
2.72	288.	2.72	257.
2.22	288.	2.22	257.
1.19	288.	1.23	258.

Module: SN 309

Before coating.		After coating.	
Voltage (Vdc)	Current (mA)	Voltage (Vdc)	Current (mA)
4.35 V	---	4.35 V	---
3.93	228. mA	3.92	211. mA
3.84	247.	3.83	227.
3.75	260.	3.74	239.
3.62	273.	3.60	250.
3.48	281.	3.47	253.
3.17	289.	3.16	254.
2.73	290.	2.72	254.
2.23	290.	2.22	254.
1.24	291.	1.36	254.

Module: SN 304

Before coating.		After coating.	
Voltage (Vdc)	Current (mA)	Voltage (Vdc)	Current (mA)
4.33 V	---	4.34 V	---
3.92	203. mA	3.91	211. mA
3.83	223.	3.83	230.
3.74	244.	3.74	244.
3.60	262.	3.60	257.
3.47	273.	3.47	265.
3.16	285.	3.16	272.
2.72	289.	2.71	274.
2.22	289.	2.22	274.
1.09	289.	1.38	274.

APPENDIX B.

IMPS and LIPS III module specifications and drawings.

Pertinent technical specifications for the integral solar cell cover modules are presented in the following sections.

Cell Output Performance:

The electrical output of the module under one sun intensity will be:

a) I_{SC} = 0.30 ± 0.02 A

b) V_{OC} = 4.3 ± 0.1 V (@28°C)

c) FF = 0.75 ± 0.15 .

Temperature transducer:

a) Wahl thin film RTD sensor, Model G105 (100Ω)

b) Source: Government Furnished Equipment (GFE)

Mounting Platform Temperature:

The module mounting platform temperature shall not exceed 150°C at any time.

Module Thermal Characteristics:

a) Solar absorptance of surfaces: 0.72 ± 0.05

b) Hemispherical emittance of emitting surfaces: 0.8 ± 0.1

Sketches of IMPS module from Interface Control Document (ICD):

(See pages 33 through 36.)

APPENDIX B (cont'd)

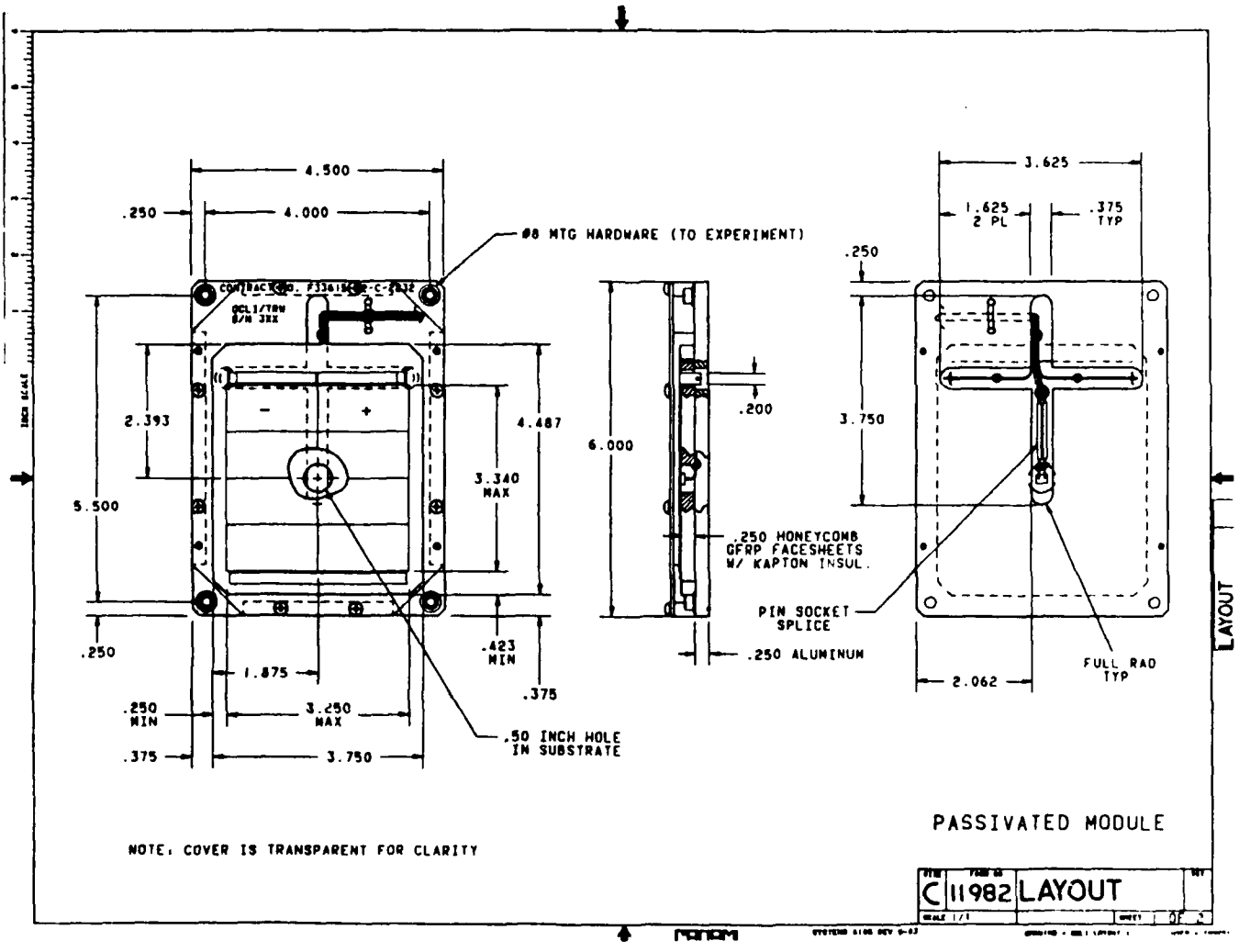

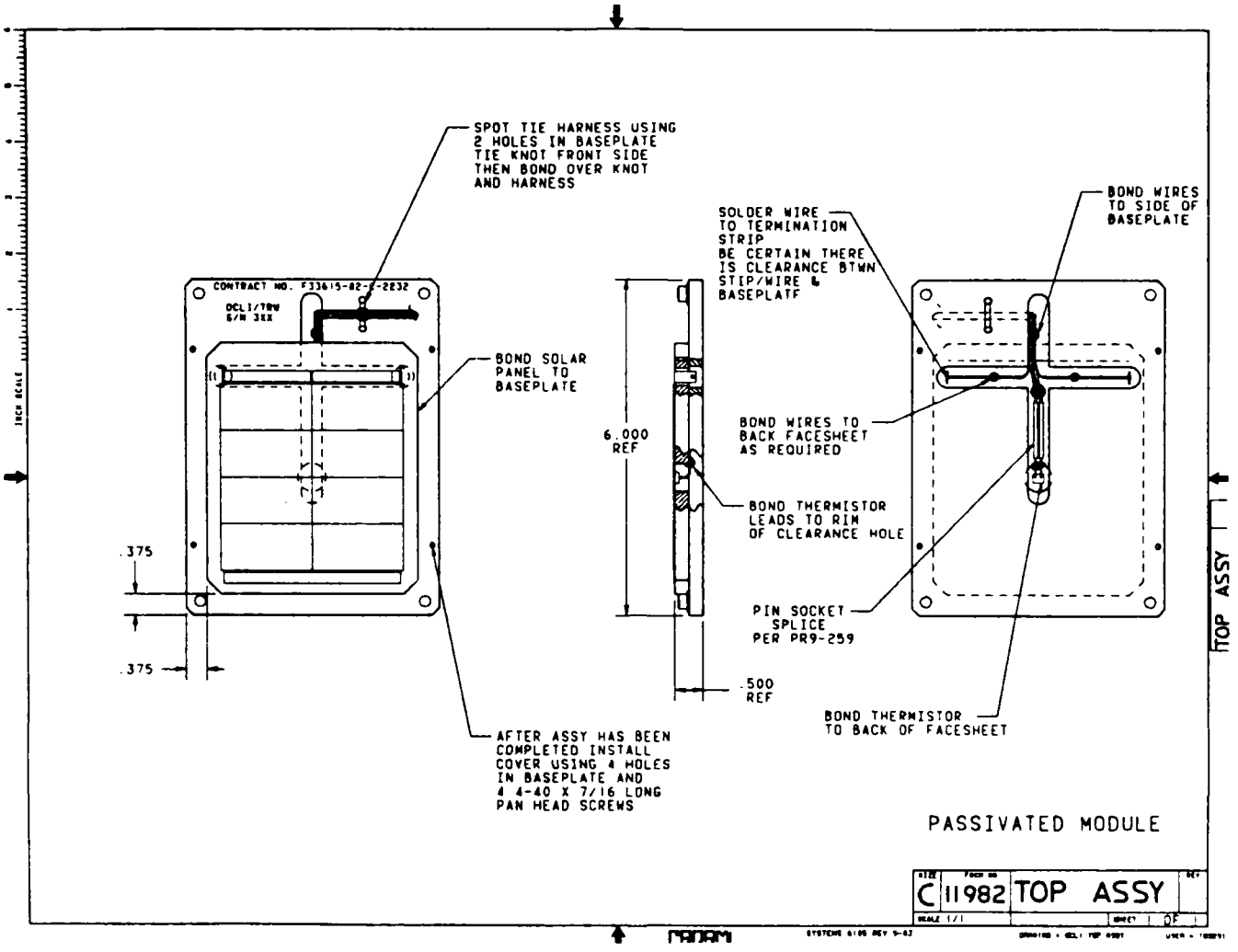
SPOT TIE HARNESS USING
2 HOLES IN BASEPLATE
TIE KNOT FRONT SIDE
THEN BOND OVER KNOT
AND HARNESS
SOLDER WIRE
TO TERMINATION
STRIP
BE CERTAIN THERE
IS CLEARANCE BTWN
STIP/WIRE &
BASEPLATE
BOND WIRES
TO SIDE OF
BASEPLATE
BOND SOLAR
PANEL TO
BASEPLATE
6.000
REF
BOND WIRES TO
BACK FACESHEET
AS REQUIRED
BOND THERMISTOR
LEADS TO RIM
OF CLEARANCE HOLE
.375
.375
PIN SOCKET
SPLICE
PER PR9-259
.500
REF
BOND THERMISTOR
TO BACK OF FACESHEET
AFTER ASSY HAS BEEN
COMPLETED INSTALL
COVER USING 4 HOLES
IN BASEPLATE AND
4 4-40 X 7/16 LONG
PAN HEAD SCREWS
TOP ASSY
PASSIVATED MODULE
C
11982
TOP ASSY

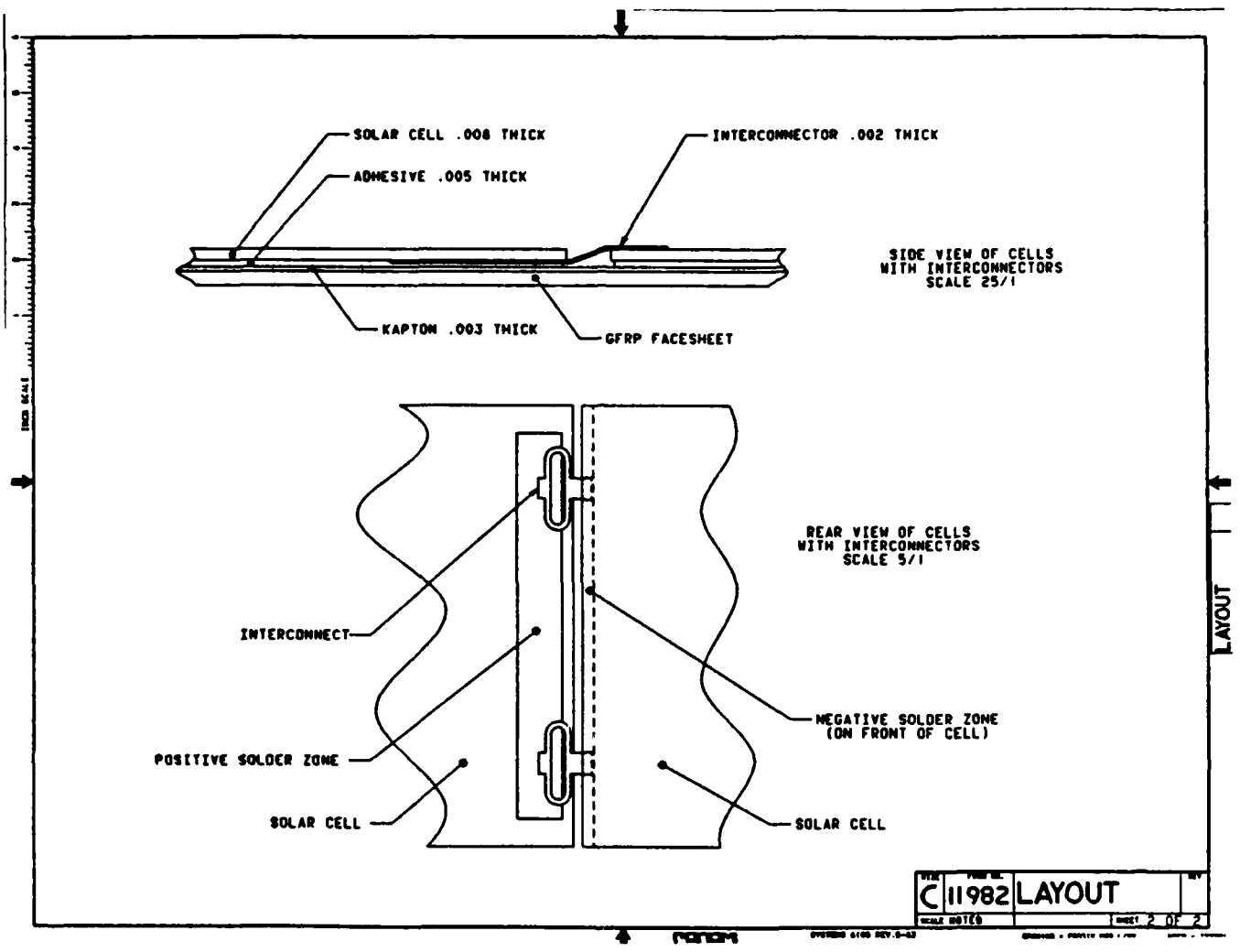
SOLAR CELL .008 THICK
ADHESIVE .005 THICK
INTERCONNECTOR .002 THICK
KAPTON .003 THICK
GFRP FACESHEET
SIDE VIEW OF CELLS WITH INTERCONNECTORS SCALE 25/1
REAR VIEW OF CELLS WITH INTERCONNECTORS SCALE 5/1
INTERCONNECT
POSITIVE SOLDER ZONE
SOLAR CELL
NEGATIVE SOLDER ZONE (ON FRONT OF CELL)
SOLAR CELL
LAYOUT
C 11982 LAYOUT
SHEET 2 OF 2

APPENDIX B (cont'd)

SIMPLIFIED SCHEMATIC

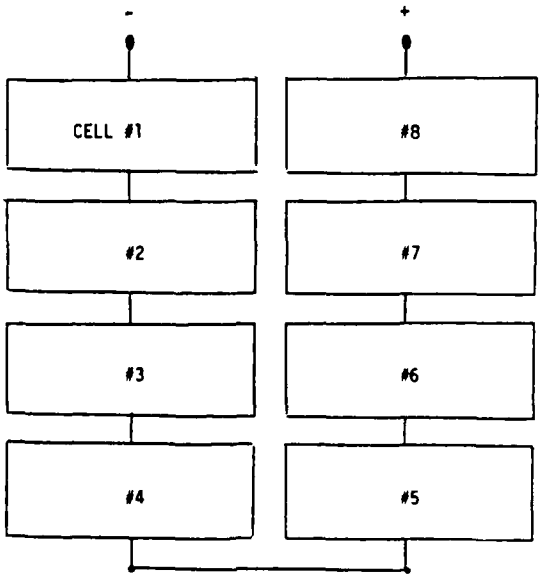

APPENDIX C

Qualification Test Specifications.

Location:

All acceptance and qualification tests were performed by TRW, Engineering and Test Division, Space and Technology Group.

Data documentation:

All test data was documented by TRW, Engineering and Test Division, Space and Technology Group.

Certification:

The TRW project manager certified that the tests were conducted and the resulting test data was obtained and documented at the time of the actual testing.

Thermal Cycling Testing:

Test: Thermal cycling of environmental test module in air or nitrogen between at least -50°C and at least +100°C for 25 cycles.

Result: Pass.

Sinusoidal Vibration Testing:

Test: The environmental test module will be exposed to swept sinusoidal vibration in all three axes to the following levels (input levels at the module base plate):

Frequency (Hz)	Qual Level
5 - 13.6	20 mm DA
13.6 - 35	7.5 $g_{0\text{-}pk}$
35 - 80	1.5 $g_{0\text{-}pk}$

Duration: Sweep up and down at 2 octaves / minute.

Result: Pass.

Random vibration test:

Test: The environmental test module will be exposed to random vibration in all three axes to the following levels (input levels at the module base plate):

A. Perpendicular to the Module Base Plate (z-axis):

Frequency (Hz)	Qual Level
20 - 50	0.025 G^2 / Hz
50 - 120	+12 dB_2 / oct
120 - 360	2.0 G / Hz
360 - 2000	-9 dB / oct
	g_{rms} = 29.6

Duration: 3 minutes.

Result: Pass.

B. Parallel to the Module Base Plate (x and y-axes):

Frequency (Hz)	Qual Level
20 - 95	0.025 G^2 / Hz
95 - 150	+9 dB_2 / oct
150 - 600	0.1 G / Hz
600 - 2000	-9 dB / oct
	g_{rms} = 8.8

Duration: 3 minutes per axis.

Result: Pass.

Flight Acceptance:

The capability of the Flight Module to withstand the launch and orbital environments was established by the following:

a) Thorough visual inspections of the Flight Module.

b) Similarity analysis between the environmental test module and the Flight module.

c) Electrical output testing of the Flight Module.

U.S. Government Printing Office: 1987 — 748-061/60641

END

3-87

DTIC